HART-II: Prediction of Blade-Vortex Interaction Loading

Joon W. Lim, Chee Tung, Yung H. Yu
Army/NASA Rotorcraft Division
Aeroflightdynamics Directorate (AMRDEC)
US Army Aviation and Missile Command
Moffett Field, California

Casey L. Burley, Thomas Brooks, Doug Boyd
NASA Langley Research Center
Hampton, VA

Berend van der Wall, Oliver Schneider
Institut für Flugsystemtechnik
Deutsches Zentrum für Luft-und Raumfahrt e.V (DLR)
Braunschweig, Germany

Hugues Richard, Markus Raffel
Deutsches Zentrum für Luft-und Raumfahrt e.V (DLR)
Gottingen, Germany

Philippe Beaumier, Joëlle Bailly, Yves Delrieux,
Office National D'Etudes et de Recherches Aerospatiales (ONERA)
Chatillon, France

Kurt Pengel, Edzard Mercker
German-Dutch Wind Tunnel (DNW)
Noordoostpolder, The Netherlands

Abstract

During the HART-I data analysis, the need for comprehensive wake data was found including vortex creation and aging, and its re-development after blade-vortex interaction. In October 2001, US Army AFDD, NASA Langley, German DLR, French ONERA and Dutch DNW performed the HART-II test as an international joint effort. The main objective was to focus on rotor wake measurement using a PIV technique along with the comprehensive data of blade deflections, airloads, and acoustics. Three prediction teams made preliminary correlation efforts with HART-II data: a joint US team of US Army AFDD and NASA Langley, German DLR, and French ONERA. The predicted results showed significant improvements over the HART-I predicted results, computed about several years ago, which indicated that there has been better understanding of complicated wake modeling in the comprehensive rotorcraft analysis. All three teams demonstrated satisfactory prediction capabilities, in general, though there were slight deviations of prediction accuracies for various disciplines.

Notations

Abbreviations

AFDD	Aeroflightdynamics Directorate
BL	Baseline
BTD	Blade Tip Deflection
DLR	German Aerospace Center
DNW	German-Dutch Wind Tunnel
HART	HHC Aeroacoustic Rotor Test
HHC	Higher Harmonic Control
MN	Minimum Noise
MV	Minimum Vibration
NASA	National Aeronautics and Space Administration
ONERA	Office National d'Etudes et de Recherches Aerospatiales

Presented at the 29th European Rotorcraft Forum (ERF), Friedrichshafen, Germany, 16-18 September 2003.

PIV	Particle Image Velocimetry
SPR	Stereo Pattern Recognition

Symbols

bpf	blade passage frequency
c_n	blade section normal force coefficient
M	Mach number
α_S	rotor shaft angle (positive aft)
θ_{3C}	cosine component of 3-per-rev pitch control
θ_{3S}	sine component of 3-per-rev pitch control
μ	advance ratio
ψ	azimuth angle

Introduction

In a major cooperative program within the existing US-German and US-French Memoranda of Understanding/Agreements, researchers from German DLR, French ONERA, NASA Langley, Netherlands DNW and the US Army Aeroflightdynamics Directorate (AFDD) conducted a comprehensive experimental program in October 2001 with a 40%, dynamically-scaled model of a BO-105 hingeless main rotor in the open-jet anechoic test section of the German-Dutch wind tunnel (DNW). This international cooperative program is the HART-II (Higher harmonic control Aeroacoustics Rotor Test) and is an extension of the HART-I program in 1994. The objective of the HART-II (Refs. 1-5) was to focus on the rotor wakes and their development. The data from this test include a total of 63000 3C-PIV (3-Component Particle Image Velocimetry) data sets, 33600 SPR (Stereo Pattern Recognition) and BTD (Blade Tip Deflection) data sets, 183 rotor balance data sets, 642 noise measurements, 157 pressure data sets. The data total approximately one terabyte (=1000 gigabytes) in size.

The US Army AFDD, NASA Langley, German DLR and French ONERA made a joint international effort for analytical predictions of Blade-Vortex-Interaction (BVI) events with HART-II measured data. The measured data for correlation included rotor blade deflections, lift ($M^2 c_n$), wake geometry, PIV velocity map, and noise data. The wind tunnel simulation in a descent flight condition was selected for comparison. The major interests were primarily for the baseline, minimum noise and minimum vibration cases. Correlation efforts focused on prediction of the lift, blade deflections, wake geometry, and noise, and consequently addressed the current status of prediction capability of the comprehensive analysis to deal with the challenging HART-II test data.

An earlier HART-I correlation study (Ref. 6) found that there was significant variation in the rotor wake prediction and that there was a strong need for more refined wake data in order to gain a better understanding of the physics of the vortex wake. Successive correlation efforts with the HART-I data revealed that accurate prediction of 3-per-rev harmonic responses of lift distribution was a very challenging task. Some adjustment in comprehensive analysis models was necessary to improve the accuracy of the prediction (Refs. 7-10), such as prescribing blade torsion with the measured data and/or vortex wake geometry iterative refinement.

In this paper, three test conditions were examined, all with a shaft angle of 5.3 degrees tilted aft: baseline case (BL), minimum noise (MN) and minimum vibration (MV) cases. The comprehensive correlation efforts from all the HART-II prediction teams were made for various disciplines including blade deflections, airloads, vortex wake and acoustics data. This paper assesses the status of prediction capability of the comprehensive rotorcraft analysis tools used by each organization.

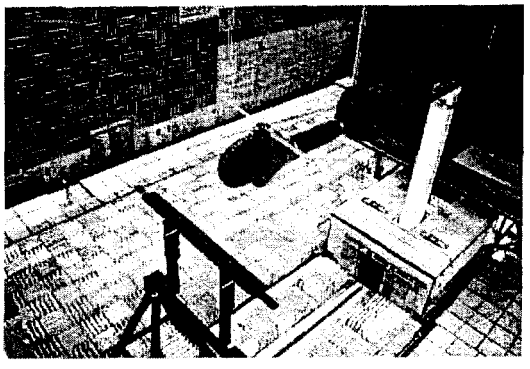

Figure 1. HART-II hingeless rotor model in the DNW wind tunnel.

Rotor Description and Test Setup

The DNW is a subsonic, closed return circuit atmospheric pressure wind tunnel with three interchangeable test sections of different sizes. HART-II was conducted in the open-jet configuration of 8m x 6m cross-sections, in the large anechoic testing hall with a volume of 52m x 30m x 20m (= 31,200 m^3). The maximum airspeed

achievable for HART-II was 85m/sec, but the airspeed for actual HART-II test was 33m/sec, equal to the advance ratio of 0.15.

The HART-II model rotor was positioned on the lateral center of the DNW test section, and 915 mm up from the longitudinal centerline (Fig. 1). This position enabled acoustic measurements using the traversing mechanism located inside of the tunnel shear layer. The newly designed rotor test rig, ROTEST II features high-frequency hydraulic rotor control actuators for the higher harmonic rotor control. The test rig contains the hydraulic drive system, the rotor balance, and the control system supported by the computer-controlled, hydraulically actuated support mechanism of the DNW.

Table 1. HART-II rotor property data

No. of blades	4
Radius	2m
Root cutout	0.44m
Chord	0.121m
Solidity	0.077
Airfoil	NACA23012mod

Table 2. HART-II blade non-rotating frequency in torsion

Blade no	Frequency [/rev]		Comments
	nonrot	rotating	
1	3.48	3.62	HELIFLOW blade
2	3.63	3.77	No Kulites
3	3.61	3.74	No Kulites
4	3.52	3.66	2nd Kulite blade

The HART-II test used a 40% Mach scaled, four-bladed hingeless BO-105 model rotor. It was aeroelastically scaled such that the model rotor blade matched the natural frequencies of the full-scale model for the first three flap, first two lead-lag and first torsion modes. Since a direct scaling cannot match the Reynolds numbers at atmospheric pressure, the blade chord was increased by 10%. The blades are rectangular with -8° of linear built-in twist and a precone of 2.5° as in the full-scale rotor, but they have a modified NACA23012 airfoil with a 5.4mm (4.46% chord) trailing edge tab. The nominal operating speed was 1041 rpm, and the hover tip Mach number was 0.641. A brief description of HART-II rotor is given in Table 1.

The reference and opposite blades were equipped with blade root pitch potentiometers, and each of the four blades had six strain gauges at the blade root: three for flap, two for lead-lag and one for torsion. The behavior of strain gauges appeared in a linear range. From a shake test, the non-rotating torsional frequencies were measured for all the blades as in Table 2. Due to its instrumentation, the reference blade showed the lowest frequency among all the blades. The rotating frequencies were calculated from the measured non-rotating frequencies.

Two blades had instrumentation with absolute pressure sensors. The reference blade was equipped with 25 pressure sensors and the preceding blade (blade no. 4) was with 26 pressure sensors. The reference blade had a leading edge sensor at five radial stations between 40% to 97% span locations, and was fully instrumented at 87% blade span with a chordwise distribution of 17 Kulites, that allowed acquisition of the sectional aerodynamic load data.

Noise measurements were made from 13 microphones mounted laterally on a traverse, located 1.3m below the tunnel centerline and equally spaced 0.45m apart from each other in the lateral direction, extending the range of -2.7m to 2.7m. During the test, the vertical position of hub center was positioned at 0.915m above the tunnel centerline, which would result in placing a noise measurement plane 2.215m below the hub center. The longitudinal and lateral positions of hub center were, respectively, 0.05m downstream and 0m from the tunnel center. The acoustics data were recorded through microphones for 100 revolutions continuously at a sample rate of 2048/rev.

There were different measurement equipment setups required during the entire program completion, and Ref. 2 summarized various methods for the measurements and their responsible organizations.

Comprehensive Analyses

The HART-II prediction teams were formed with the US Army AFDD, NASA Langley, German DLR and French ONERA. Pre-test calculations were made for guidance in finding the BVI locations during the measurement as well as sanity

check for the pressure data. Each prediction team member generated pre-test predictions of vortex locations prior to the wind tunnel test and the PIV measurement windows were placed based on these predictions. The methodologies for the comprehensive analyses from each prediction team were based on somewhat different algorithms, and a brief description for their comprehensive analyses is given here.

US Army AFDD/NASA Langley

The US Army AFDD and NASA Langley formed a joint US team, and they employed the Comprehensive Analytical Model of Rotorcraft Aerodynamics and Dynamics (CAMRAD II) (Refs. 11-12) for calculation of the lift, blade response, and wake geometry. The structural model was based on finite nonlinear beam elements, and the fully coupled, flap, lead-lag and torsion nonlinear equations of motion were solved for wind tunnel trim. Each blade consisted of 10 nonlinear beam elements and 16 aerodynamic panels. The pitch bearing was located at 3.75% radial location with control stiffness of 400 Nm. The calculated blade frequencies were 1.11, 0.78 and 3.65 per rev for flap, lead-lag and torsion, respectively.

The unsteady aerodynamics model used for the prediction was based on the modified ONERA EDLIN (Equations Differentielles Lineaires) theory (Ref. 11), which was available in the CAMRAD II code. For the vortex wake modeling, multiple free vortex wake trailers were convected downstream. These trailers were consolidated into a smaller number of rolled-up vortex line filaments using the trailed vorticity moment for scaling the rate of rollup. After certain aging of the rollup process multiple bundling of the vortex trailers occurred not only at the blade tip but also at the inboard locations. Due to a large memory requirement for a refined vortex wake model, the trim was achieved with a 15^{o} azimuthal time step, and then post-processed to a 1.5^{o} steps for correlation. The noise was calculated using the WOPWOP mod code (Ref. 13) based on Ffowcs Williams-Hawkings equation, as a post-processor to the CAMRAD II code.

German DLR

The German DLR rotor analysis code, S4 was used for computation of rotor and hub dynamics and able to calculate high-resolution blade airloads for acoustic post-processing. The S4 code consisted of aerodynamics, structural dynamics and induced velocity modules, and was based on the modal method. Unsteady, nonlinear aerodynamics including Mach, yaw and dynamic stall effects are taken into account.

The blade dynamics were represented by their flap, lead-lag and torsion mode shapes of the rotor. For description of the rotor downwash, there were various options available: a constant, linear or non-uniform inflow distribution according to Mangler-Squire, a prescribed wake geometry following Beddoes, and a free-wake model (Ref. 14). Due to modification of the downwash wake geometry when active control techniques are applied, a free-wake model is commonly thought to be mandatory for nonlinear rotor simulations. However, the semi-empirical prescribed wake model, which takes into account the low frequency harmonic rotor loading (2-6/rev) for computation of wake deformations, was used (Ref. 15) and thus represented a compromise between accuracy and computational efficiency. The steady aerodynamics were represented by a semi-empirical math model that allows computation of unsteady aerodynamic coefficients including dynamic stall and yawed flow effects as well as time-varying velocity (Ref. 16). Flap aerodynamics in attached and separated flow was also available (Ref. 17).

The aeroacoustics code, Aeroacoustic Prediction System based on Integral Method (APSIM), has been developed at DLR Institute of Aerodynamics and Flow Technology for prediction of rotor or propeller noise radiated in the free far-field (Ref. 18). The methodology of APSIM was based on both Ffowcs Williams-Hawkings and Kirchhoff formulations, and only linear sound propagation was taken into account. The APSIM code computes the acoustic pressure at any desired observer location, is a post-processor to airload prediction codes, and is presently capable of accepting blade pressure distributions from DLR UPM-MANTIC (Main and tail rotor interaction code) (Ref. 19) for main/tail rotor interaction noise prediction.

French ONERA

The numerical methods used at ONERA consist in five main steps (Ref. 20). HOST (Ref. 21) is an aeroelastic code (developed by Eurocopter) that trims the rotor taking into account aerodynamic, inertial and elastic forces and moments on the blades. The aerodynamic model is based on the lifting line method. In the METAR code (Ref. 22), the wake model is defined by a prescribed helicoidal geometry described by vortex lattices. A

coupling between HOST and METAR is made until convergence is achieved on induced velocities at the rotor disk level, so that the rotor trim accounts for vortical wake and blade flexibility.

The prescribed wake geometry obtained by HOST/METAR is then distorted by using a free wake analysis code, MESIR (Ref. 23). In this free wake analysis code, a lifting line method similar to that in HOST/METAR is used. The blade motion calculated in HOST is given to the MESIR code. In the wake deformation process, the whole wake structure is distorted, and wake geometry iterations are continued until circulation convergence is achieved after a few iterations.

An intermediate step between wake geometry and blade pressure calculation is introduced using the MENTHE code (Ref. 24). During the roll-up process of the vortices, MENTHE identifies the portion of vortex sheets that the MESIR code calculated as having sufficiently strong intensity to roll-up. These rolled sheet regions constitute interacting vortices.

Blade pressure distribution is then calculated by the unsteady singularity method, ARHIS (Ref. 25). This code assumes that the flow around the rotor is inviscid and incompressible. It performs 2D-by-slices calculations. Subsonic compressibility effects are included by means of Prandtl-Glauert corrections combined with local thickening of the airfoil. In addition, finite span effects are introduced through an elliptic-type correction of the pressure coefficients. The interacting vortices are modeled as freely convecting and deforming clouds of vortex elements. The main advantage of this method is its ability of taking into account the vortex deformation during strong blade-vortex interactions.

The noise radiation is computed by the PARIS code (Ref. 26), using pressure distribution calculated from ARHIS. The PARIS code is based on the Ffowcs Williams-Hawkings equations and predicts the loading and thickness noise. It uses a time domain formulation. An efficient spanwise interpolation method has been implemented, which identifies the BVI impulsive events on the signatures generated by each individual blade section.

Results and Discussion

Selected test conditions were for the baseline (BL), minimum noise (MN) and minimum vibration

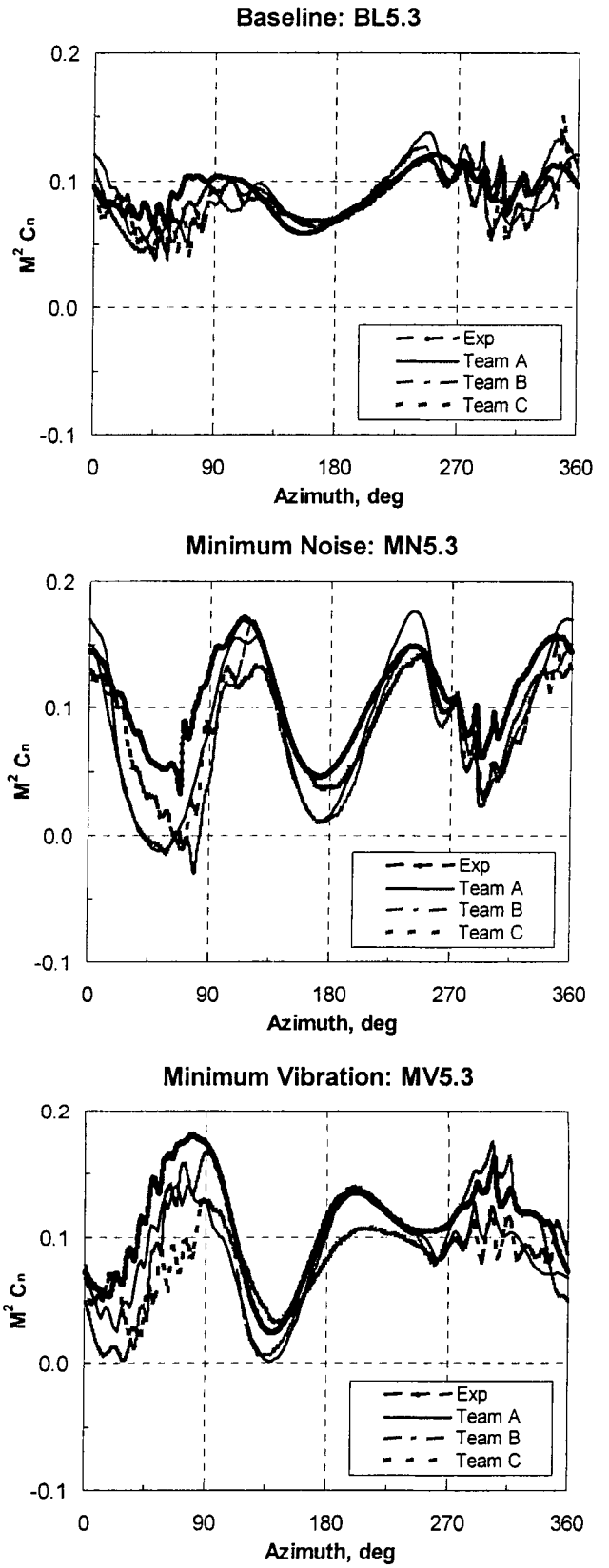

Figure 2. Lift predictions ($M^2 c_n$) at the 87% blade span for the BL, MN, and MV cases at $\mu = 0.15$.

(MV) cases. All these were limited to the cases with a shaft tilt of 5.3 degrees aft. For the trimmed condition, the rotor was trimmed to the thrust and the hub aerodynamic moments (pitching and rolling). The 3/rev pitch control input was added for the minimum noise and minimum vibration cases, and then re-trimmed to reach the trim targets. Table 3 describes 3 per rev pitch control inputs and their measured trim targets. The θ_{3C} and θ_{3S} are respectively the cosine and sine components of 3-per-rev higher harmonic pitch input. Note that positive moments for the hub rolling and pitching are the advancing side up and the fuselage nose up, respectively.

Table 3. HART-II rotor trim data for selected cases

Cases	BL5.3	MN5.3	MV5.3
θ_{3C}	--	0.41°	-0.79°
θ_{3S}	--	-0.70°	0.00°
Thrust, N	3,250	3,303	3,286
Roll moment, Nm	-18	-31	-16
Pitch moment, Nm	-15	-30	-29

Sectional Airload

Sectional blade airloads were obtained by integrating the measured blade surface pressures along the airfoil chord at the fully instrumented radial stations. All measured pressure data were acquired at a rate of 2048-per-rev for 60 continuous revolutions. Figure 2 shows comparison of the non-dimensional lift (normal force), $M^2 c_n$ along with an azimuth angle (ψ) for the blade span location of 87%. The measured data (Exp) exhibited a large 3-per-rev lift for the BL case, and these 3-per-rev lifts became stronger for the MN and MV cases due to the 3-per-rev pitch inputs. The measured data also revealed strong BVI induced loadings in the advancing and retreating sides. Predicted lifts by all three predictions well captured the trend of 3-per-rev harmonics of the measured data, although the peak-to-peak lift value predicted by team C was substantially lower for the MV case. Good capability of predicting the 3-per-rev lift was a key issue in the HART-I correlation efforts (Refs. 6-10), and this might be overcome due to improved capability of vortex wake modeling. The azimuthal step sizes that prediction teams used for their analyses were different, ranging from 0.3 to 2 degrees, and these refined step sizes allowed to capture well the BVI loadings both on the advancing and retreating sides. Overall, all lift predictions were good for 3-per-rev harmonics of airloads and the BVI loading.

Blade Deflections

The blade deflections were measured optically by Stereo Pattern Recognition technique (SPR) (Ref. 4). Figure 3 shows time histories of the lead-lag, flap and elastic torsion at the blade tip, and the spanwise elastic torsion distribution is at an azimuth of 60°. The lead-lag deflection is positive toward the leading edge, and the flap deflection is the deflection without precone angle and is defined positive up. The elastic torsion is a torsional deflection without pitch control and pre-twist, and is positive for the leading edge up.

It was observed that the lead-lag tip deflections were almost identical for the BL, MN and MV cases, which implied that the 3-per-rev pitch control difference of about 0.8° in magnitude between the baseline and other cases was not large enough to generate a sizable change in drag force and correspondingly change in lead-lag moment. The predicted trends of lead-lag deflections were similar to the measured data but there were constant offsets between the measured data and predicted results. The largest offset occurred between the measured data and the team C prediction, was about 30% of the blade chord length, and it might be partially due to poor or incorrect understanding of the blade geometry. For the flap, all the predicted deflections at the blade tip were in good agreement with the measured data.

The elastic torsion is considered significant to get good prediction of lift. Since the torsion variation is directly related to the angle of attack and accordingly the lift, the phase and peak-to-peak values of elastic torsion are essential for accurate prediction. As shown in Fig. 3, phase predictions of elastic torsion from all three teams were in good agreement with the measured data for the BL, MN and MV cases. However, all the teams poorly predicted the peak-to-peak values for the BL case. The team C predictions for the MN and MV cases were about a half of the peak-to-peak measured data, and less than other predictions. Therefore, one would expect the lower peak-to-peak value of the predicted lift for team C, as seen in Fig. 2. Lower mean elastic torsion was also observed in the team B prediction, compared with the measured data, and

this difference could be compensated for by larger trim controls to ensure correct rotor thrust. The predicted spanwise distribution of elastic torsion is shown at an azimuth of 60°. It is observed that the measured elastic torsion data may not satisfy the hingeless boundary conditions of zero slope near

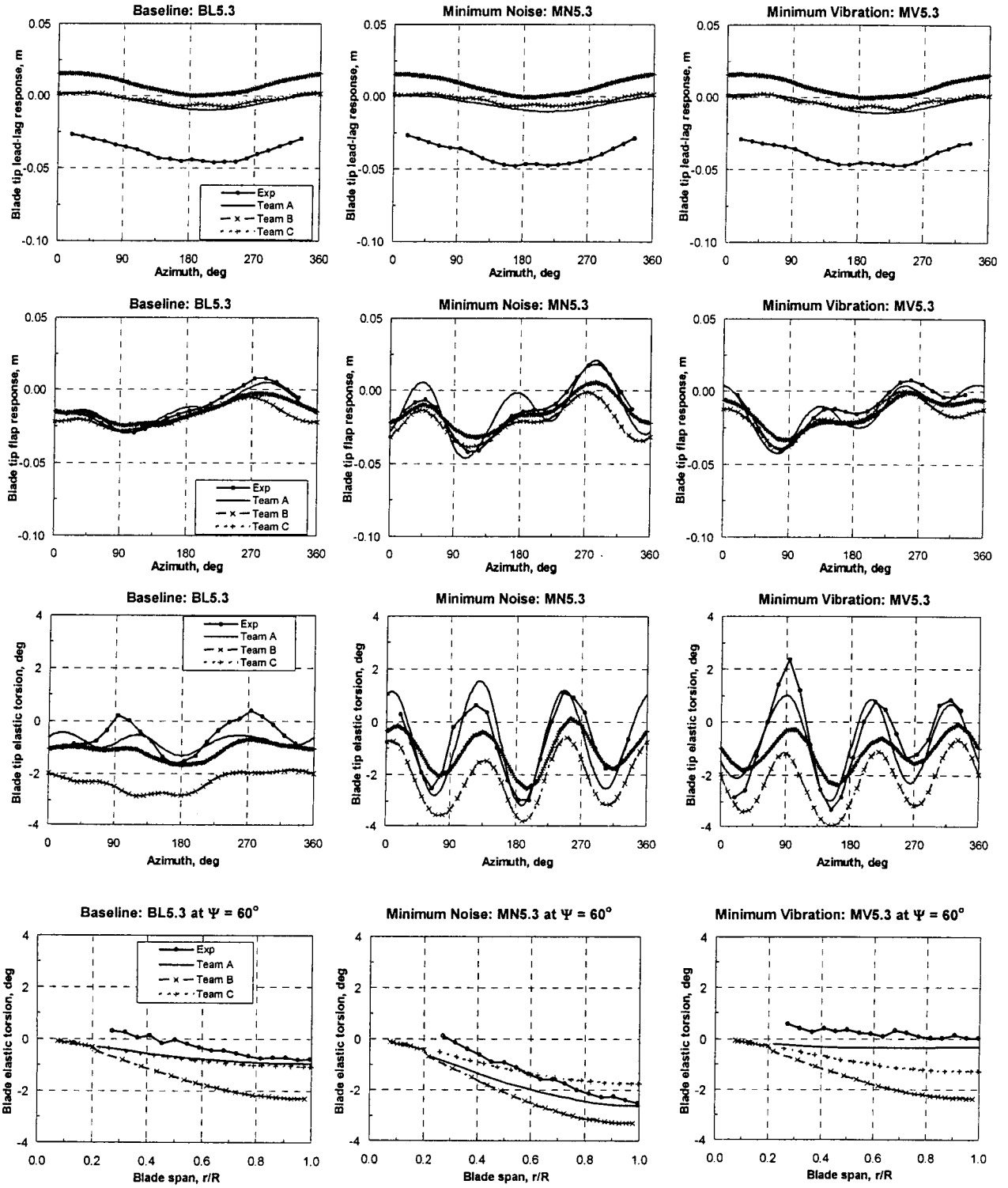

Figure 3. Time histories of blade lead-lag, flap and elastic torsion at the blade tip and the spanwise elastic torsion at an azimuth of 60 degrees for the BL, MN, and MV cases at $\mu = 0.15$.

the blade root for all three cases. The measured data depicted was for an actual azimuth of 64°, and this 4° difference was due to the instrumentation signal delay. The team B prediction of the spanwise elastic torsion drifted lower along the blade span from others, and this would be expected since the time history of the elastic torsion at the blade tip indicated that the team B predicted result was lower at an azimuth of 60° by at least one degree, compared with other data.

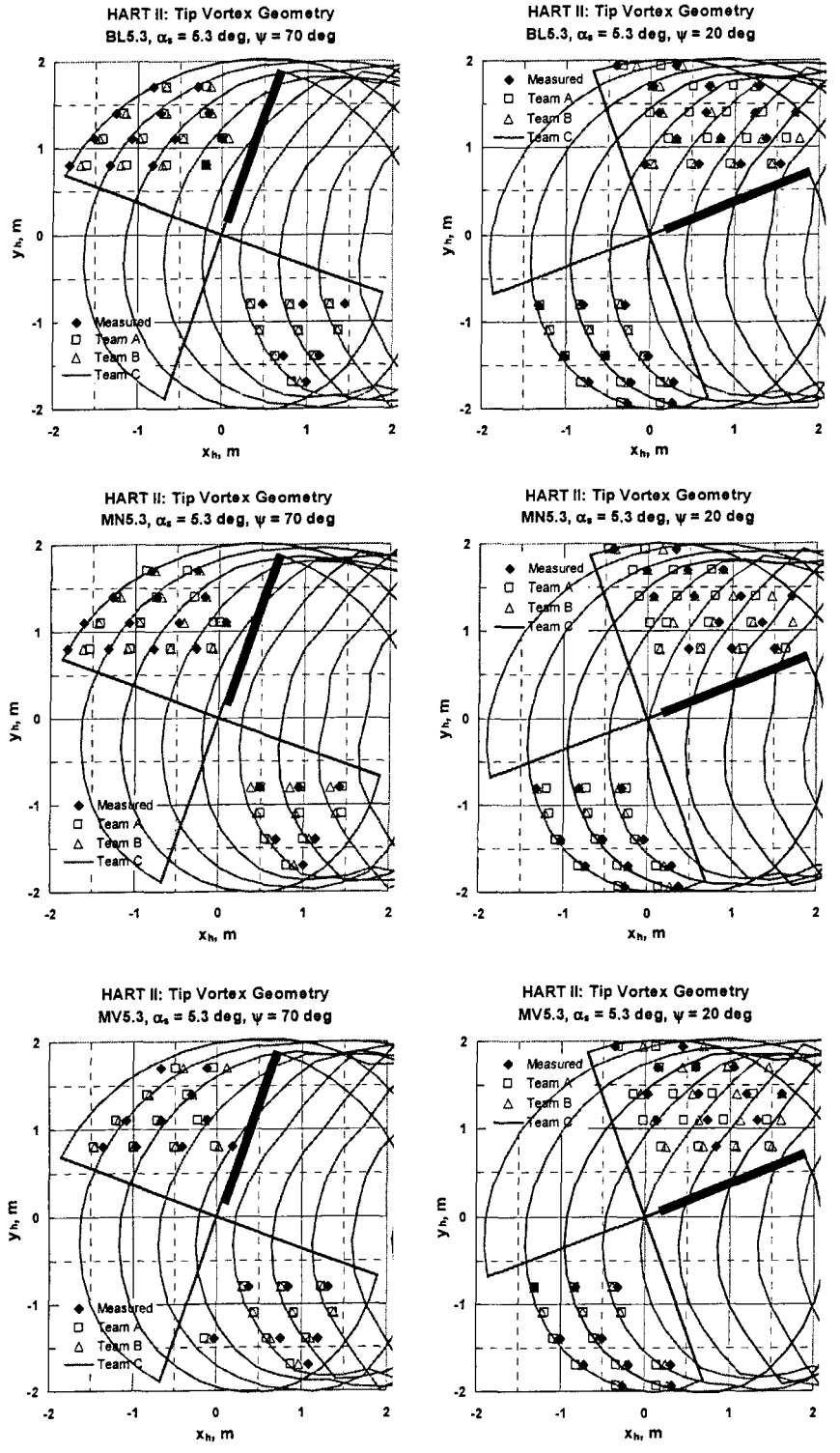

Figure 4. Top view prediction of tip vortex wake geometries of the HART-II rotor blade for the BL, MN and MV cases.

Tip Vortex Wake Geometry

Extensive measurements of the rotor wake were obtained by a 3-component Particle Image Velocimetry (PIV) technique (Ref. 6), including tip vortex geometry and vortex structures over the entire rotor disk. From the PIV vector maps, details of the vortices, such as core size, strength, and circulation, are determined as a function of wake age. The PIV measurements were obtained for about 50 locations on both the advancing and retreating side with the reference blade at $\psi = 20°$ and 70°. Figure 4 shows a top view of predicted tip vortex geometry for the BL, MN and MV cases. For the measured data, the PIV measurement window locations were shown, instead of actual vortex locations. The data are shown in the hub coordinate system, and the z-axis is defined positive up along the shaft axis. The reference blade location for the measured data was actually lagged by 3.5° due to the instrumentation response time delay. The solid lines are the team C predictions, and are intended to show the overall trend of the tip vortex wake geometries.

The predicted tip vortex wake geometries in the first quadrant of the rotor were well predicted by team B, while the results from teams A and C were lagged for all

three cases. These lags were not found in the second quadrant. However, initial positions of the tip vortex roll-up were shown excessively inboard for teams A and B. Predictions in the third quadrant were very good for all three teams, but deteriorated in the fourth quadrant.

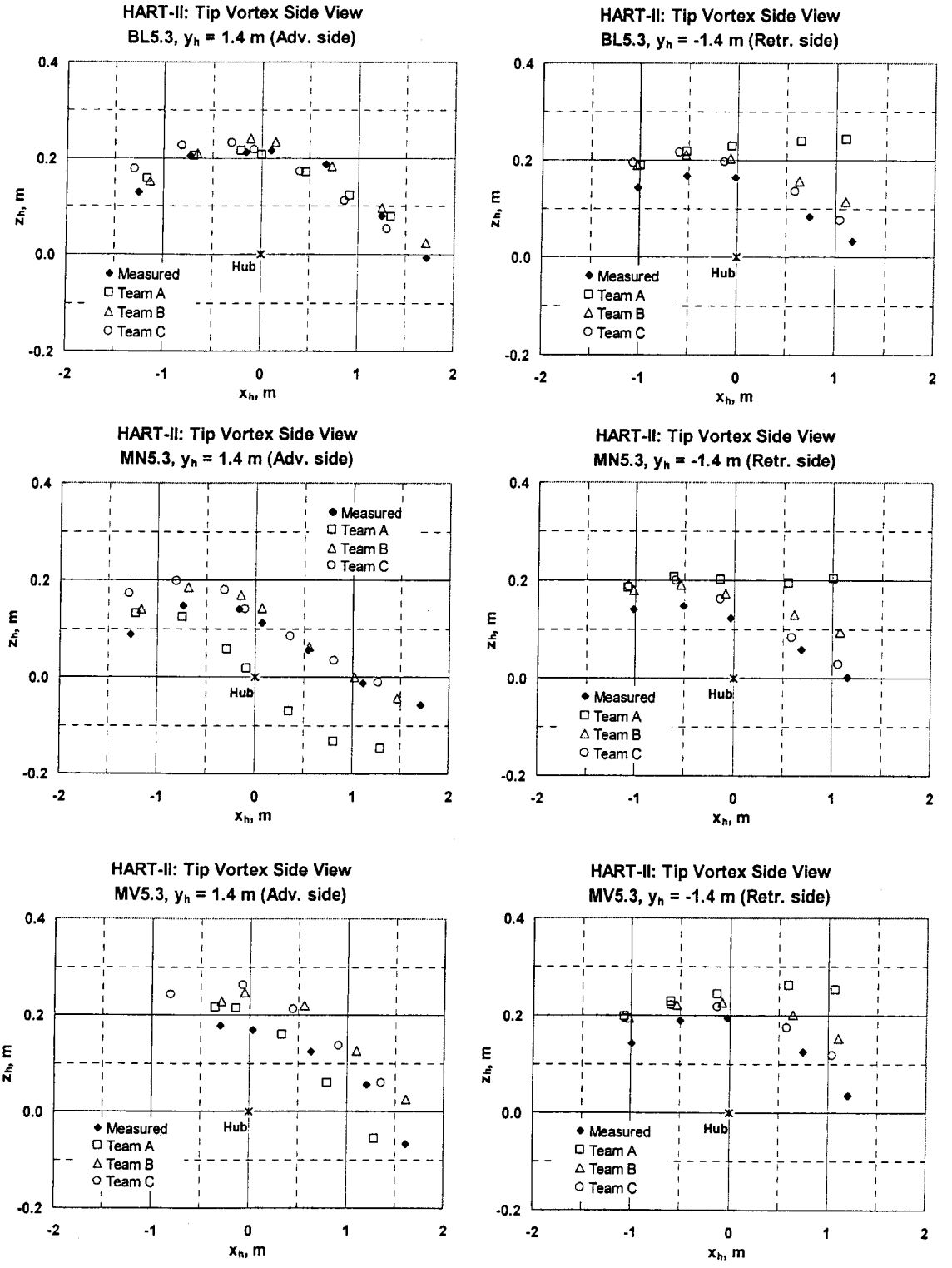

Figure 5. Side view prediction of tip vortex wake geometries of the HART-II rotor blade for the BL, MN and MV cases.

The side view of the tip vortex wake geometries is shown in Fig. 5. The projected planes are parallel to the aircraft longitudinal axis, and located 1.4m from the hub center for both the advancing and retreating sides. The positive z-value is above the hub plane along the shaft, and the undeformed blade tip position is 0.087m from the hub plane due to precone angle of 2.5°. The vortices were initiated from the reference blade at azimuths of 20° and 70°, as in Fig. 4, and predictions were obtained by capturing vortices when they were crossing through the projected plane.

For the BL case, all three teams predicted well the vertical positions of tip vortices in the second quadrant (advancing side), but when they moved toward the first quadrant the longitudinal movement of tip vortices apparently slowed for teams A & C as seen in the top view, Fig. 4. The team B predicted result was in good agreement with the measured data. The team A prediction became substantially underpredicted on the advancing side for the MN case, while seemed slightly better for the MV case. The teams B and C predicted results were close to each other, and compared well with the measured data. Especially, the team B predicted well the longitudinal movement of the tip vortices.

Consistent trends from all three predictions on the retreating side were shown for the BL, MN and MV cases. The team A prediction consistently overpredicted the vertical positions of the tip vortices. The team B and C predictions were in good agreement with the trend of the measured data, and the team C prediction was very good.

For an analysis of the vortex properties, the coordinates and velocity field have to be transformed into the local PIV coordinate system from the wind tunnel coordinate system. From tangential velocity fields, the vortex core size is determined from the distance between two maximum tangential velocities. The development of vortex structures, such as core size, roll-up and aging process, along the downstream over the three rotor revolutions were carefully investigated from this database. The typical velocity field map was obtained from the PIV measurement, as shown in Fig. 6. Images were the center-aligned, and the averaged velocity field was calculated using all 100 available images for each PIV location. The vortex in the position 22 was initiated from the third blade while the reference blade was at $\psi = 20°$, and after one revolution of aging it encountered the projection plane at y = 1.4m. The origins of the PIV measurement windows in the hub coordinate system are shown in Table 4. The BL case demonstrated a strong vortex and the corresponding velocity field was in clear circular motion due to vorticity. The MN and MV cases exhibited a half the magnitude of the BL vorticity, and correspondingly the velocity field was weaker.

Table 4. The origins of the PIV measurement windows for selected cases

Cases	x_h, m	y_h, m	z_h, m
BL5.3 (Dpt 998)	1.25	1.4	0.08
MN5.3 (Dpt 963)	1.11	1.4	-0.01
MV5.3 (Dpt 867)	1.61	1.4	-0.07

Finally, noise level validation is considered as a final stage by post-processing the airloads data.

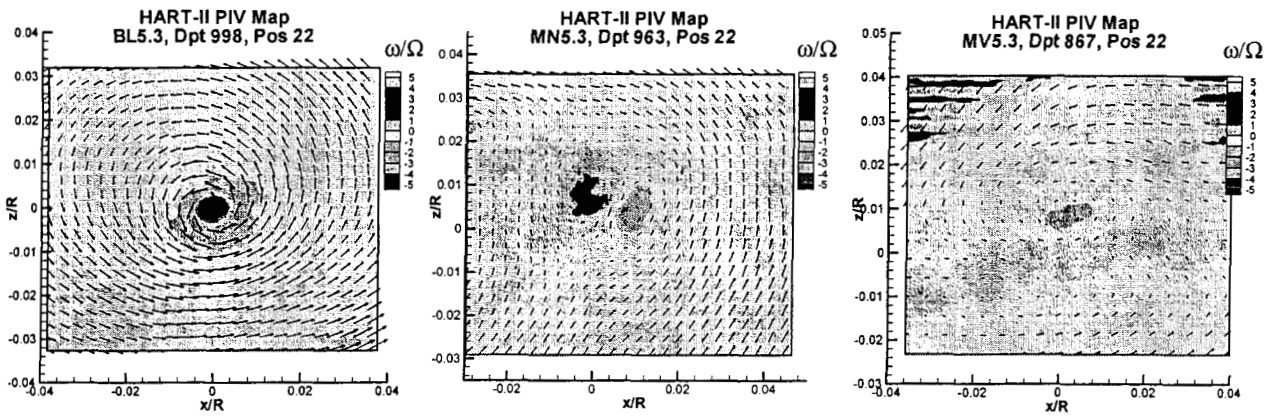

Figure 6. PIV map of the measured data at the measurement position 22 for the BL (Dpt 998), MN (Dpt 963), and MV (Dpt 867) cases.

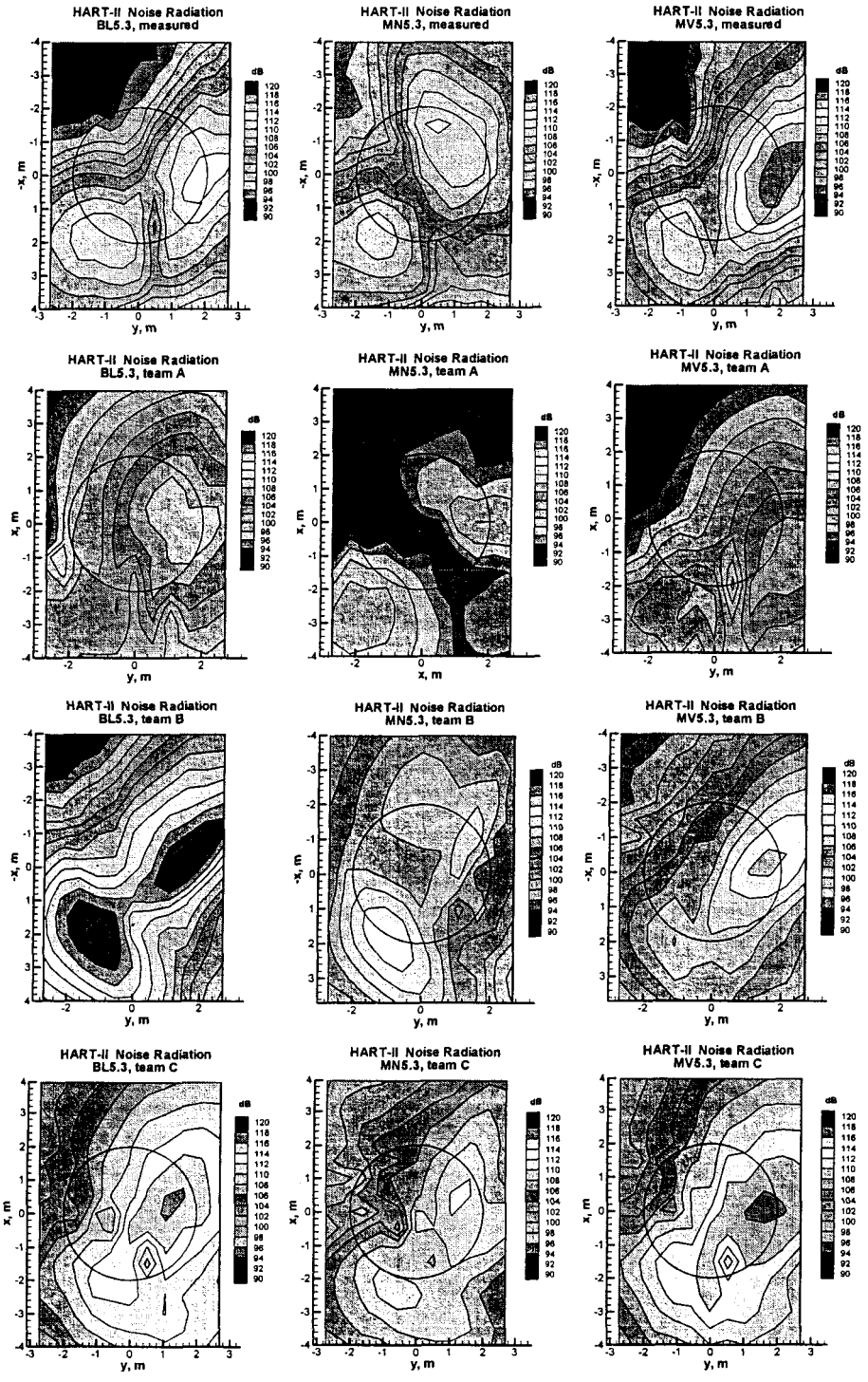

Figure 7. Comparison of mid-frequency (6-40 bpf) noise radiation for the BL, MN and MV cases.

Figure 7 shows comparison of the mid-frequency (6-40 bpf) noise level predictions for the BL, MN and MV cases. The microphones were equally spaced 0.45m apart from each other and placed in the plane 2.215m below the hub center. As observed from the measured data, the noise level in the BL case was strong on the advancing side and quiet in the front of the rotor. In order to achieve minimum noise the noise intensity on the advancing side became weaker and was moved forward as shown in the MN case. Interestingly, the MV case showed that the noise intensity on the advancing side was even stronger than the BL case and its center was moved back. Accuracy of noise prediction capabilities was very different for various prediction teams. Overall, The team A prediction was consistently poor for three cases. The team C showed improved prediction over team A, and the team B prediction was good. Because good predictions of airloads were achieved from all the prediction teams as shown in Fig. 2, this variation was not expected.

Conclusions

Correlations of HART-II rotor data were made under a joint international cooperative program. Three flight conditions were selected for this study - the baseline, minimum noise and minimum vibration conditions in descent flight. Various disciplines were correlated from the blade dynamics, airloads, vortex wake geometry and noise. It may be concluded on the basis of the present results that US Army AFDD, NASA Langley, German DLR and French ONERA provided satisfactory results. In some areas, agreement with measured data was not acceptable. In some cases, due to the preliminary nature of the measured data or known experimental

uncertainties, disagreement would result, and in other cases the comprehensive analyses were likely responsible for the discrepancies.

To summarize key findings in the individual areas of correlation, the following additional comments are made:

1. Lift predictions from all prediction teams were good for the BL, MN and MV cases. Strong BVI phenomenon in the BL case was well predicted.

2. Predicted results of blade deflections were fair-to-good for waveform. Compared with the measured data, all teams showed constant offsets in the mean values for the lead-lag and elastic torsion. There was uncertainty in the measured elastic torsion data whether or not it would satisfy the hingeless boundary conditions near the blade root.

3. Tip vortex wake geometries in the top view were reasonably predicted by all prediction teams, except for the first quadrant of the rotor. The vertical positions of tip vortex geometries were well predicted by some teams.

4. The comparisons in noise radiation patterns are generally acceptable.

References

1. Raffel, M., Richard, H., Schneider, G., Klinge, F., Ehrenfried, K., Pengel, K., Feenstra, G., "Recording and Evaluation Methods of PIV Investigations on a Helicopter Rotor Model," 11th International Symposium on the Application of Laser Techniques applied to Fluid Mechanics, Lisbon, Portugal, July 2002, paper 8.4.

2. van der Wall, B.G., Junker, B., Burley, C.L., Brooks, T., Yu, Y.H., Tung, C., Raffel, M., Richard, H., Wagner, W., Mercker, E., Pengel, K., Holthusen, H., Beaumier, P., Prieur, J., "The HART-II Test in the LLF of the DNW-a Major Step towards Rotor Wake Understanding," 28th European Rotorcraft Forum, Bristol, England, September 2002.

3. Burley, C. L., Brooks, T.F., van der Wall, B.G., Richard, H., Raffel, M., Beaumier, P., Lim, J.W., Yu, Y.H., Tung, C., Pengel, K., "Rotor Wake Vortex Definition and Validation from 3-C PIV HART-II Study," 28th European Rotorcraft Forum, Bristol, England, September 2002.

4. Pengel, K., Mueller, R., van der Wall, B.G., "Stereo Pattern Recognition – the technique for reliable rotor blade deformation and twist measurement," Heli-Japan 2002, AHS International Meeting on Advanced Rotorcraft Technology and Life Saving Activities, Utsunomiya, Japan, November 2002.

5. Yu, Y.H., Tung, C., van der Wall, B.G., Pausder, H., Burley, C., Brooks, T., Beaumier, P., Delrieux, Y., Mercker, E., Pengel, K., "The HART-II Test: Rotor Wakes and Aeroacoustics with Higher-Harmonic Pitch Control (HHC) Inputs - The Joint German/French/Dutch/US Project," American Helicopter Society 58th Annual Forum, Montreal, Canada, June 2002.

6. Tung, C., Gallman, J.M., Kube, R., Wagner, W., van der Wall, B., Brooks, T.F., Burley, C.L., Boyd, D. D., Rahier, G., and Beaumier, P., "Prediction and Measurement of Blade-Vortex Interaction Loading," 1st Joint CEAS/AIAA Aeroacoustics Conference, Munich, Germany, June 1995.

7. Rahier, G., and Delrieux, Y., "Blade-Vortex Interaction Noise Prediction Using a Rotor Wake Roll-up Model," *Journal of Aircraft*, Vol.34, No. 4, pp 522-530, July-August 1997.

8. Lim, J.W., and Tung, C., "2GCHAS Prediction of HART Blade-Vortex Interaction Loading," American Helicopter Society Technical Specialists' Meeting for Rotorcraft Acoustics and Aerodynamics, Williamsburg, VA, October 1997.

9. Lim, J.W., Tung, C., Yu, Y.H., "Prediction of Blade-Vortex Interaction Airloads with Higher-Harmonic Pitch Controls Using the 2GCHAS Comprehensive Code," *Journal of Pressure Vessel Technology,* Transaction of the ASME, Vol.123, No.4, pp.469-474, November 2001.

10. Wachspress, D.A., and Quackenbush, T.R., "Wake Model Requirements for Prediction of BVI Airloads," American Helicopter Society Technical Specialists' Meeting for Rotorcraft Acoustics and Aerodynamics, Williamsburg, VA, October 1997.

11. Johnson, W., "Rotorcraft Aerodynamics Models for a Comprehensive Analysis," American Helicopter Society 54th Annual Forum Proceedings, Washington, D.C., May 1998.

12. Johnson, W., "Influence of Wake Models on Calculated Tiltrotor Aerodynamics," presented at the American Helicopter Society Aerodynamics, Acoustics, and testing and Evaluation Technical Specialists Meeting, San Francisco, CA, January 2002.

13. Burley, C.L., Brooks, T.F., Marcolini, M.A., Brand, A.G., and Conner, D.A., "Tiltrotor Aeroacoustic Code (TRAC) Predictions and Comparisons with Measurement," *Journal of American Helicopter Society*, April 2000, pp. 80-89.

14. Brentner, K.S., Burley, C.L., and Marcolini, M. A., "Sensitivity of Acoustic Predictions to Variation of Input Parameters," *Journal of American Helicopter Society*, Vol. 39, No. 3, July 1994.

15. Splettstoesser, W.R., Schultz, K.J., van der Wall, B.G., Buchholz, H., Gembler, W., Niesl, G., "The Effect of Individual Blade Pitch Control on BVI Noise - Comparison of Flight Test and Simulation Results," 24th European Rotorcraft Forum, Marseille, France, September 1998.

16. van der Wall, B.G., "An analytical Model of Unsteady Profile Aerodynamics and its Application to a Rotor Simulation Program," 15th European Rotorcraft Forum, Amsterdam, Netherlands, September 1989.

17. van der Wall, B.G., "The Influence of Variable Flow Velocity on Unsteady Aerodynamic Behavior," 15th European Rotorcraft Forum, Avignon, France, September 1992.

18. van der Wall, B.G., Geissler, W., "Experimental and Numerical Investigations on Steady and Unsteady Behaviour of a Rotor Airfoil with a Piezoelectric Trailing Edge Flap," 55th American Helicopter Society Forum, Montreal, Canada, May 1999.

19. Yin, J., "Acoustic Prediction Using Ffowcs-Williams/Hawkings Formulation Based on CAMRAD Aerodynamic Airload Input," DLR 129-2001/17, Braunschweig, Germany, September 2001.

20. Yin, J., Ahmed, S., "Helicopter main-rotor/ tail-rotor interaction," *Journal of the American Helicopter Society*, Vol. 45, No. 4, pp293-302, October 2000.

21. Beaumier, P., Spiegel, P., "Validation of ONERA Aeroacoustic Prediction Methods for Blade-Vortex Interaction Using HART Tests Results," 51st Annual Forum and Technology Display of the AHS, Fort Worth, TX, May 1995.

22. Benoit B., Dequin A.M., Kampa K., Grunhagen W., Basset P.M., Gimonet B., "HOST, A General Helicopter Simulation Tool for Germany and France," 56th Annual Forum of the American Helicopter Society, Virginia Beach, VA, May 2000.

23. Arnaud G., Beaumier P., "Validation of R85/METAR on the Puma RAE flight tests," 18th European Rotorcraft Forum, Avignon, France, September 1992.

24. Michéa B., Desopper A., Costes M., "Aerodynamic Rotor Loads Prediction Method with Free Wake for Low Speed Descent Flight," 18th European Rotorcraft Forum, Avignon, France, September 1992.

25. Rahier G., Delrieux Y., "Improvement of Helicopter Rotor Blade-Vortex Interaction Noise Prediction using a Rotor Wake Roll-Up Model," 16th AIAA Aeroacoustic Conference, Munich, Germany, June 1995.

26. Spiegel P., Rahier G., Michéa B., "Blade-Vortex Interaction Noise: Prediction and Comparison with Flight and Wind Tunnel Tests," 18th European Rotorcraft Forum, Avignon, France, September 1992.

27. Spiegel P., Rahier G., "Theoretical Study and Prediction of BVI Noise Including Close Interactions," AHS Technical Specialists Meeting on Rotorcraft Acoustics and Fluids Mechanics, Philadelphia, PA, October 1991.